IOPscience iopscience.iop.org

Home Search Collections Journals About Contact us My IOPscience

Advances in modeling of lower hybrid current drive

This content has been downloaded from IOPscience. Please scroll down to see the full text.

2016 Plasma Phys. Control. Fusion 58 044008

(http://iopscience.iop.org/0741-3335/58/4/044008)

View the table of contents for this issue, or go to the journal homepage for more

Download details:

IP Address: 211.86.158.38
This content was downloaded on 05/06/2017 at 02:29

Please note that terms and conditions apply.

You may also be interested in:

Propagation of the lower hybrid wave in a density fluctuating scrape-off layer (SOL)
M Madi, Y Peysson, J Decker et al.

Modelling of the EAST lower-hybrid current drive experiment using GENRAY/CQL3D and TORLH/CQL3D
C Yang, P T Bonoli, J C Wright et al.

Experimental and modeling uncertainties in the validation of lower hybrid current drive
F M Poli, P T Bonoli, M Chilenski et al.

High-power lower hybrid current drive in TORE SUPRA
Y Peysson, the TORE SUPRA Team and Y Peysson

High power lower hybrid current drive experiments in the Tore Supra tokamak
Y. Peysson and Tore Supra Team

Comparative modelling of lower hybrid current drive with two launcher designs in the Tore Supra tokamak
E. Nilsson, J. Decker, Y. Peysson et al.

RF current drive and plasma fluctuations
Yves Peysson, Joan Decker, L Morini et al.

Ray-tracing and Fokker–Planck modelling
F Imbeaux and Y Peysson

Chapter 6: Steady state operation
C. Gormezano, A.C.C. Sips, T.C. Luce et al.

IOP Publishing Plasma Physics and Controlled Fusion

Plasma Phys. Control. Fusion **58** (2016) 044008 (14pp) doi:10.1088/0741-3335/58/4/044008

Advances in modeling of lower hybrid current drive

Y Peysson[1], J Decker[1,5], E Nilsson[1], J-F Artaud[1], A Ekedahl[1], M Goniche[1], J Hillairet[1], B Ding[2], M Li[2], P T Bonoli[3], S Shiraiwa[3] and M Madi[4]

[1] CEA, IRFM, 13108, Saint-Paul-Les-Durance Cedex, France
[2] ASIPP, 230031 Hefei, People's Republic of China
[3] PSFC MIT, MA-02139, Cambridge, USA
[4] AUB, Beirut, Lebanon

E-mail: yves.peysson@cea.fr

Received 26 June 2015, revised 26 November 2015
Accepted for publication 2 December 2015
Published 18 February 2016

Abstract

First principle modeling of the lower hybrid (LH) current drive in tokamak plasmas is a longstanding activity, which is gradually gaining in accuracy thanks to quantitative comparisons with experimental observations. The ability to reproduce simulatenously the plasma current and the non-thermal bremsstrahlung radial profiles in the hard x-ray (HXR) photon energy range represents in this context a significant achievement. Though subject to limitations, ray tracing calculations are commonly used for describing wave propagation in conjunction with Fokker–Planck codes, as it can capture prominent features of the LH wave dynamics in a tokamak plasma-like toroidal refraction. This tool has been validated on several machines when the full absorption of the LH wave requires the transfer of a small fraction of power from the main lobes of the launched power spectrum to a tail at a higher parallel refractive index. Conversely, standard modeling based on toroidal refraction only becomes more challenging when the spectral gap is large, except if other physical mechanisms may dominate to bridge it, like parametric instabilities, as suggested for JET LH discharges (Cesario *et al* 2004 *Phys. Rev. Lett.* **92** 175002), or fast fluctuations of the launched power spectrum or 'tail' LH model, as shown for Tore Supra (Decker *et al* 2014 *Phys. Plasma* **21** 092504). The applicability of the heuristic 'tail' LH model is investigated for a broader range of plasma parameters as compared to the Tore Supra study and with different LH wave characteristics. Discrepancies and agreements between simulations and experiments depending upon the different models used are discussed. The existence of a 'tail' in the launched power spectrum significantly improves the agreement between modeling and experiments in plasma conditions for which the spectral gap is large in EAST and Alcator C-Mod tokamaks. For the Alcator C-Mod tokamak, the experimental evolution of the HXR profiles with density suggests that this model is valid up to a line-averaged density of $\overline{n}_e \simeq 1.0 \times 10^{+20}$ m^{-3}, a statement that is confirmed by simulations of the HXR scaling law with density. While simulations with GENRAY/CQL3D codes have ascribed the fast decrease of the HXR emission with density to parasitic absorption in the scrape-off layer by collisional damping, an alternative interpretetation based on an enhanced refraction as the LH wave propagates in the vicinity of the X-point is provided by C3PO/LUKE codes. The consequences for the predictions of LH current in ITER are discussed.

Keywords: 52.50.Sw, 52.55.Wq, 52.25.Gj

(Some figures may appear in colour only in the online journal)

[5] Present address: EPFL, CRPP, F-13108 Lausanne, Switzerland

 © 2016 IOP Publishing Ltd Printed in the UK

1. Introduction

Even if the lower hybrid (LH) wave system has not yet been selected to be among the first heating systems installed on ITER tokamak, its experimentally proven high efficiency for driving a toroidal current makes it one of the most attractive methods for this purpose [1–3]. Consequently, an active research is maintained on existing machines, with the goal to demonstrate the effectiveness of this method in ITER-relevant operating conditions for off-axis shaping of the current density profile. In this context, numerous studies have been carried out, for example, investigating the long-range coupling capability of advanced LH antennae able to withstand high power fluxes, in particular during ELMy H-mode regimes [4–6].

Although encouraging results have been obtained for successful use of the LH wave in the ITER tokamak, recent studies have pointed out the importance of the edge plasma characteristics on the core absorption of the LH wave that could change the standard picture of the first principles LH wave modeling that has been carried out up to now [7–12]. The non-thermal bremsstrahlung in the hard x-ray range of photon energy (HXR) used as a measure of the current drive efficiency is found to fall off rapidly with the density, a scaling law that is ascribed to parasitic absorption of the LH wave by collisional damping in the dense surrounding scrape-off layer outside the separatrix [9, 13–15]. Besides, in plasma conditions for which the LH wave absorption is weak, it is shown that introducing fast fluctuations of the power spectrum at the separatrix leads to an improved agreement between modeling and observations in the Tore Supra tokamak, in particular concerning the HXR profile. In order to retrieve the experimental phenomenology, the transfer of power from the narrow spectrum excited by the antenna to a broad spectral tail must exceed 50% [16].

Measurement of the non-thermal bremsstrahlung provides an almost direct insight into the build-up of the non-thermal electron velocity distribution pulled out from the thermal bulk to high kinetic energies by resonant interaction between electrons and the LH wave [17]. This diagnostic is therefore crucial to assess the capability of the LH wave to be used as a non-inductive current source in ITER from experiments performed in existing machines, in combination with magnetic measurements. In this context, several HXR cameras with a high spatial resolution have been installed for LH current drive studies, most of them using cadmium telluride (CdTe) based detectors whose energy response is well adapted for this purpose. This feature greatly simplifies multimachine and multicode comparisons[6] [18–20].

The modeling effort performed with GENRAY/CQL3D and C3PO/LUKE ray tracing/Fokker–Planck codes is reported [21–25], on the basis of the experimental results obtained on three tokamaks, Tore Supra, EAST and Alcator C-Mod [14, 16, 26–29]. This set of machines represents an interesting ensemble to assess the level of universality of the LH modeling, regarding the differences in aspect ratio, plasma shape, operational densities and magnetic fields, and the various types of antennae and frequencies that are used.

In order to highlight the challenges in LH wave modeling, especially with the tools used in this study, conditions of propagation and absorption of the LH wave in a magnetized plasma are first recalled in section 2. Even if the ray tracing formalism has intrinsic limitations for describing the propagation of the LH wave related to the WKB approximation, this tool coupled to a 3D Fokker–Planck solver (1D in configuration space, 2D in velocity space) is particularly flexible for calculating the electron velocity distribution function from first principles and its moments for direct comparisons between modeling results and experimental data by synthetic diagnostics. Coupled ray tracing and Fokker–Planck calculations are based on underlying assumptions that are described in section 3. A discussion of the ray tracing robustness based on fullwave calculations is proposed [30]. In section 4, specificities of the C3PO/LUKE and GENRAY/CQL3D codes that could impact both predictions and interpretation are discussed. Results of the LH current drive simulations are gathered in section 5. After recalling the main conclusions drawn from previous LH modeling, new simulations of LH discharges in EAST and Alcator C-Mod tokamaks are presented, using the recently developed fast fluctuating power spectrum model at the separatrix also named the 'tail' LH model [16]. This heuristic model, which is implemented only in C3PO/LUKE code, has been successfully used in reproducing several parametric dependencies of Tore Supra LH experiments and line-integrated HXR profiles even if plasma conditions correspond to a weak LH wave power absorption. Regarding the encouraging results concerning the Tore Supra tokamak, the role played by the spectral 'tail' in the launched power spectrum is investigated for the LH wave in the EAST and Alcator C-Mod tokamaks, using the same set of simulation parameters of the 'tail' LH model as for Tore Supra. The range of validity of the 'tail' LH model is investigated from the evolution of the HXR profile with density on the Alcator C-Mod tokamak, and in light of these results, the interpretation of the scaling law of the HXR emission with the line-averaged density is addressed. The consequences for LH current drive in ITER are discussed.

2. Propagation and absorption of the lower hybrid wave

The physics of the LH wave in tokamak plasmas is a wide domain, and covering all its details is beyond the scope of this study [31]. Here, the most important concepts useful for understanding modeling challenges are summarized.

Efficient methods for current drive in hot magnetized plasmas may be achieved by accelerating electrons to velocities largely exceeding the thermal level, a direct consequence of the $|\mathbf{v}|^{-3}$ dependence of the Coulomb collision frequency, where $\mathbf{v}$ is the electron velocity [32]. The rf wave at a frequency ω slightly higher than the LH resonance frequency has the interesting property to propagate in the plasma with a large parallel phase velocity $v_{\phi\parallel}/v_{\mathrm{th}} \gg 1$ allowing to pull out a tail

[6] The EAST tokamak has been recently equipped with a 20 chord CdTe camera.

of fast electrons from the thermal bulk by Landau damping. Here, $v_{\phi\|}$ is related to the parallel component $n_\|$ of the refractive index $\mathbf{n} = c\mathbf{k}/\omega$ by the usual relation $v_{\phi\|} = c/n_\|$ where $n_\| = \mathbf{n}\cdot\mathbf{B}/\|\mathbf{B}\|$, $\mathbf{B}$ is the local magnetic field, $\mathbf{k}$ the wave vector and $v_{\rm th}$ is the thermal velocity. The electrons that interact with the LH wave must fulfill locally the resonance condition $v_\| \approx v_{\phi\|}$ in the plasma. By accelerating electrons along the magnetic field lines, the LH wave is therefore particularly well suited for non-inductive current drive in tokamaks, as observed experimentally [31].

At the considered frequencies[7], the LH wave does not propagate in vacuum and must be excited by a complex array of waveguides placed in the scrape-off layer (SOL) [33]. Different techniques are considered, like a full phasing grill in Alcator C-Mod and fully (passive) active multijunctions FAM (PAM) in Tore Supra and EAST [5, 34, 35]. For ITER, the PAM concept is considered, thanks to its capability to withstand a high heat load for long pulse operation. With a lower density cut-off and an electric field with a higher parallel component, the 'slow'-wave branch is always used in tokamak experiments, allowing an efficient transfer of power from the wave to the electrons by Landau damping[8].

The far-field spectral characteristics of the LH wave in front of the antenna are given by the launched power spectrum $P(n_{\|0})$ which is a distribution of narrow Gaussian-like lobes with the parallel refractive index $n_{\|0}$, their relative amplitudes depending upon the phasing between waveguides[9]. Their half widths $\Delta n_{\|0}$ at e^{-1}result from the Fourier transform of the wave electric field pattern in the SOL, taking into account the finite size of the antenna along the toroidal direction [38]. Since $\Delta n_{\|0}/n_{\|0} \ll 1$, each lobe may be considered as a quasi-plane wave [39], which has important consequences for the type of propagation model used in LH current drive simulations, and for the wave-particle interaction model that is crucial for the wave absorption. These points are discussed in sections 3 and 4. In order to keep the injected power density at an acceptable technological level, especially for long pulse operation, antennas have several poloidal rows of waveguides. This characteristic has important consequences on the wave absorption regarding the high sensitivity of the wave refraction to the inhomogeneity of the magnetic field in tokamaks. Full-wave calculations show that each row is almost independent spectrally as far as magnetic field lines have a small tilt with respect to the toroidal direction in front of the antenna. With the appropriate antenna phasing, most of the power is launched by a single narrow lobe with a low $|n_{\|0}|$ such that co-current is generated[10]. The antenna directivity defines the fraction of the LH power that contributes to co- or counter-current. The part of the power spectrum which drives a counter-current corresponds generally to lobes with smaller amplitude and higher $|n_{\|0}|$. Since the wave interacts with less energetic electrons, the corresponding current is usually small. Nevertheless, this part of the launched power spectrum must be fully considered for accurate current drive calculations [27].

In order to reduce the fraction of fusion power that must be recycled for current drive and current profile control by the LH wave, it is useful to maximize the current drive efficiency by increasing $v_{\phi\|}$ or equivalently, by shifting the main lobe $|n_{\|0}^{(0)}|$ in $P(n_{\|0})$, down to the lowest possible value $|n_{\|a}| \propto \omega_{pe}/\Omega_{ce} \propto \sqrt{n_e}/B$ corresponding to the Stix–Golant accessibility criterion, where ω_{pe} and Ω_{ce} are the electron plasma and cyclotron frequencies respectively, n_e is the electron density and $B \equiv \|\mathbf{B}\|$ [36]. Indeed, in cylindrical geometry, the wave cannot propagate across the plasma layer where $|n_{\|0}^{(0)}| \leqslant n_{\|a}$ and reach the hot core of the plasma as it bounces between the inner caustics and the edge cut-off until it is absorbed, with a mode conversion between the 'slow' and 'fast' branches of the cold plasma dispersion relation [40]. However, this criterion is no longer global in a toroidal geometry, as the index of refraction $n_\|$ evolves as the wave propagates in the plasma, a consequence of the poloidal inhomogeneity of the magnetic field. Therefore, even if $|n_{\|0}^{(0)}| \leqslant n_{\|a}$, the wave may propagate inward as far as $|n_\|| \geqslant n_{\|a}$ locally. Nevertheless, when $n_{\|a}$ is close to $|n_{\|0}^{(0)}|$ at the plasma edge, the penetration of the LH wave may be difficult, even in a toroidal magnetic configuration, until the $n_\|$ upshift becomes large enough. In this regime, the current drive efficiency is usually poor, especially if the periphery of the plasma is very cold and dense, since a significant fraction of wave power may be lost by parasitic absorption [3, 15]. The magnetic configuration of the plasma has therefore an important role on the wave dynamics, especially in regions characterized by a high variation of poloidal field B_p with the poloidal angle, where the poloidal mode number m strongly increases, since $|n_\||$ is roughly proportional to m, as shown in figure 1 [24].

As the wave propagates, the ratio $v_{\phi\|}/v_{\rm th}$ evolves, and when the condition $v_{\phi\|}/v_{\rm th} \sim 4$ is locally satisfied, the linear absorption on a Maxwellian distribution becomes strong and almost all the LH power is transferred to resonant electrons by Landau interaction [32, 36, 41]. Therefore, a downshift of the phase velocity is necessary for the LH to be absorbed in the plasma if $v_{\phi\|0}^{(0)}/\widehat{v}_{\rm th} \gg 1$, as it is the case in all existing machines, where $v_{\phi\|0}^{(0)}$ is the initial phase velocity associated to the main lobe $n_{\|0}^{(0)}$ in the launched power spectrum. The value $\widehat{\cdot}$ is taken at the center of the plasma so $\widehat{v}_{\rm th}$ is the core thermal velocity. Conversely, if $v_{\phi\|0}^{(0)}/\widehat{v}_{\rm th} \leqslant 1$, as in standard LH scenarios in ITER tokamak, a downshift of the phase velocity is not necessary for the LH to be absorbed in the plasma [3]. The variations of $v_{\phi\|}$ may result from an upshift of $|k_\||$ by toroidal refraction, but also from non-linear processes which lead to a broadening of the frequency spectrum [42]. At a fixed LH frequency, the condition of strong linear absorption corresponds to the condition $|n_\|| \simeq n_{\|L}$, where $n_{\|L} \simeq c/(4v_{\rm th})$. The diverted plasma is a particularly favorable configuration for this strong

[7] For typical tokamak plasmas, the LH resonance frequency falls in the GHz domain.

[8] The LH wave dynamics is assumed to be described principally by the cold plasma dispersion relation [36]. In this case, two propagation modes with a different polarization exist, which are named the 'slow'-wave and 'fast'-wave branches respectively. Thermal corrections that can be taken into account usually have a marginal influence as long as the excited frequency ω is far enough from the LH resonance frequency in the plasma [37].

[9] The total launched LH power $P_{\rm tot}$ is defined as $P_{\rm tot} = \int_{-\infty}^{-\infty} P(n_{\|0})dn_{\|0}$.

[10] The sign of $n_{\|0}$ depends on the relative direction of the plasma current and $\mathbf{B}$

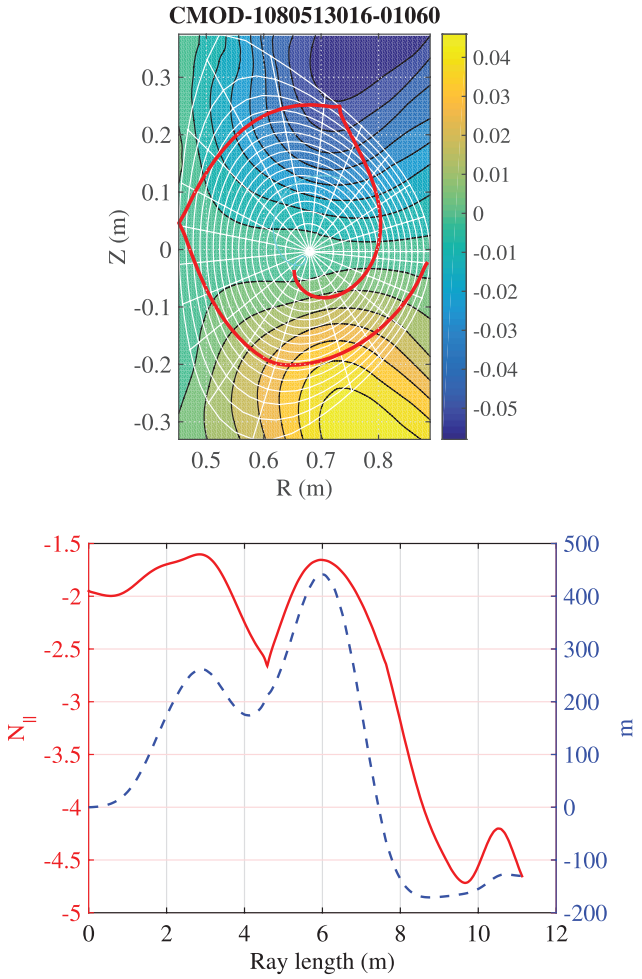

Figure 1. Ray dynamics for the LH wave in the Alcator C-Mod diverted discharge #1080513016 at $t = 1.06$ s. In the top figure, the contour plot of the toroidal MHD equilibrium (white) is drawn over the contour plot of $\Upsilon = P\partial P/\partial\theta$, where $P = B_p/B$. Blue and yellow regions correspond to large values of Υ. When the ray enters these regions, the variation of the dispersion relation with the poloidal angle becomes very large, leading to an important modification of the poloidal mode number m and $n_\parallel$ as shown in the bottom figure. In conjunction with a reflection of the wave at the separatrix, this leads to a full off-axis absorption by Maxwellian electrons.

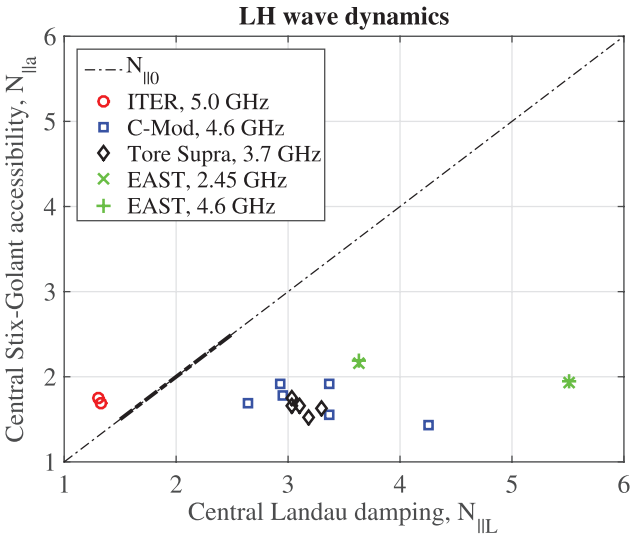

Figure 2. Regimes of the LH wave dynamics as a function of the central Landau damping and Stix–Golant accessibility condition. Results for Alcator C-Mod, EAST, Tore Supra LH experiments considered in this paper are indicated as well as the reference scenarios II and IV for ITER. The dotted–dashed line represents the $\left|n_{\parallel 0}^{(0)}\right|$, and the thick dotted–dashed line the domain of $\left|n_{\parallel 0}^{(0)}\right|$ effectively excited by existing LH antennas. ITER parameters correspond to strong absorption for the LH wave (single pass), while for all existing tokamaks, LH wave absorption is weak (multiple passes). With $\left|n_{\parallel 0}^{(0)}\right| = 2$, T_{e0} must exceed 7.5 keV for strong damping and accessible regime in existing machines.

upshift as compared to plasma with circular poloidal cross-sections, because the LH wave propagation is more tangent to the magnetic flux surfaces after a reflection near an X-point as shown in figure 1. Finally, the $|n_\parallel|$ upshift is supposed to be not bounded by a KAM surface, i.e. that the condition $(B_p/B)(\omega_{pe}/\omega) > 1$ holds everywhere in the plasma [43]. This is usually the case in most existing tokamaks and for ITER too, except for a few machines with large aspect ratio operating at very low plasma current and electron density [40, 44].

The ordering between $\left|n_{\parallel 0}^{(0)}\right|$, $\widehat{n}_{\parallel a}$ and $\widehat{n}_{\parallel L}$ leads to define several regimes for the LH wave dynamics. As shown in figure 2, for the range of $1.5 \leqslant \left|n_{\parallel 0}^{(0)}\right| \leqslant 2.5$ that can be excited by standard LH antennas, the condition $\left|n_{\parallel 0}^{(0)}\right| \geqslant \widehat{n}_{\parallel L}$ of strong absorption for the LH wave is never achieved in existing tokamaks while it is for ITER as far as $\left|n_{\parallel 0}^{(0)}\right| \geqslant 1.8$. Therefore, none of the LH experiments in existing machines have been performed in conditions close to ITER operating conditions, that may considerably weaken the extrapolation capability of simulations to reactor-grade plasmas. The closest ITER-relevant LH experiments have likely been performed in the JET tokamak, for the shot number #53429 analyzed in [42]. Nevertheless, even the central electron temperature reaches about 8 keV, such that $n_{\parallel L} \simeq 2.3$; this value did not make this experiment fully ITER-relevant regarding the criterion developed in the present paper, since the launched power spectrum peaks at $\left|n_{\parallel 0}^{(0)}\right| \simeq 1.8$. Indeed, for usual plasma parameters, the condition of propagation and absorption of the LH wave corresponds to the accessible weak absorption regime $\widehat{n}_{\parallel a} \leqslant \left|n_{\parallel 0}^{(0)}\right| \leqslant \widehat{n}_{\parallel L}$, which requires an upshift of $|n_\parallel|$ (or downshift of $v_{\phi\parallel}$) for a full damping of the LH wave. A variety of physical mechanisms have been suggested to bridge the spectral gap defined as $n_{\parallel L} - \left|n_{\parallel 0}^{(0)}\right|$, and since $n_\parallel$ varies always in a torus as a consequence of the poloidal inhomogeneity, the toroidal refraction in the plasma core has been considered as a reference mechanism for this purpose [37]. Nevertheless, it may fail when the spectral gap is large in high aspect ratio machines, and alternative mechanisms may predominate [40, 44]. The broadening of the frequency spectrum by parametric instabilities whose non-linearity makes the process power dependent may also contribute [45]. It is important to note that the width of the spectral gap has important consequences on the validity of numerical tools that are used to describe the dynamics of the LH wave in the plasma.

3. Modeling of the lower hybrid current drive

For the range of $\left|n_{\|0}^{(0)}\right|$ used in existing machines, the parallel wavelength is a few centimeters, much shorter than the gradient scale length L of the dielectric tensor and the machine size. The ray tracing formalism for calculating $n_\|$ evolution in the plasma is therefore natural, as long as the Wentzel–Kramers–Brillouin (WKB) and well-collimated beam approximations are valid, which can be expressed by the inequality $\lambda \ll d \ll L$, where λ is the wavelength and d is the beam size[11] [24, 46]. However, if the ray tracing can capture important features of the LH wave dynamics in a toroidally magnetized plasma, in particular refraction, its conditions of applicability are not always well satisfied along the wave trajectory, especially if it reaches the edge cut-off or in the presence of a caustic where individual rays converge (the focusing effect) [30]. At these points, the WKB approximation fails, and in principle full-wave calculations must be performed, which represents a considerable numerical challenge due to the very large ratio L/λ [30, 40, 47]. In addition, the concept of wavefront must be always valid to fulfill the assumptions used to derive the ray equations. Since toroidicity induces Hamiltonian chaos in the ray motion, the ray tracing has in principle lost its physical meaning if wave absorption takes place after an integration time exceeding the maximal Liapunov exponent, which characterizes the rate of separation of infinitesimally close trajectories [24]. Such a problem is particularly critical when power absorption of the LH wave is very weak [16].

Despite these important potential limitations, ray tracing calculations coupled to Fokker–Planck calculations (RTFP), which allows to describe the formation of a tail of fast electrons by Landau damping from characteristics of the LH wave at the antenna, are still widely used and are almost standard for simulating LH current drive experiments. Indeed, the numerical flexibility of this type of tool makes it particularly attractive, especially for integrated modeling, where coupling RTFP with solvers of the transport equations and the toroidal MHD equilibrium must be self-consistently considered [48]. As long as the LH wave undergoes only a few reflections from the low density cutoff at the plasma edge before being fully absorbed, predictions of the LH power absorption using ray tracing may be considered as reasonably accurate, thanks to the remarkable agreement found between ray tracing and full-wave calculations [30]. From the latter, the concept of ray remains indeed valid far from the cut-off region, and the specular reflexion may be applied despite the local failure of the WKB approximation around the cut-off layer [49]. Therefore, if the wave absorption takes place well away from the cut-off layer, a condition which is almost always satisfied in realistic LH experiments, few reflections at the plasma edge may not represent in principle a major problem in the code predictions, provided a wavefront still exists. The existence of a caustic is a more challenging difficulty, as it is located rather inward in the plasma, and the structure of the wavefield in this region may be important for calculating power absorption of the LH wave. Modified WKB techniques that still follow ray trajectories but account for diffractional spreading can capture this effect. By considering the semiclassical dynamics of wave packets, it is thus possible to build an accurate solution for the wavefield in the vicinity of a caustic, but even if this method is attractive, it has also several downsides, like the initialization of the wavepacket [49]. Though the exact wavefield structure is not correctly reproduced by standard eikonal techniques, the quasilinear selfconsistency between the wavefield and the electron distribution function may smooth out the error, making this problem less problematic than it could be. Nevertheless, with a lack of fullwave modelling regarding experiments considered in the manuscript, the performed ray tracing and Fokker–Planck study can only provide a guess of the $n_\|$ spectral change produced by the toroidicity effect, besides additional physical mechanisms.

4. Code description

Calculations presented in this paper have been carried out with C3PO/LUKE and GENRAY/CQL3D RTFP codes. The C3PO code is a generic 3D ray tracing[12] while LUKE is a solver of the 3D linearized relativistic bounce-averaged electron Fokker–Planck equation (1D in configuration space, 2D in momentum space) [23, 24]. Both codes use the same curvilinear coordinate system (ψ, θ, ϕ), where ψ is the label of nested magnetic flux surfaces in the tokamak plasma, θ and ϕ are the poloidal and toroidal angles respectively. The LUKE code is itself coupled to the quantum-relativistic bremsstrahlung synthetic diagnostic R5-X2 for calculating the non-thermal HXR emission [17]. The GENRAY code is a generic 2D ray tracing for describing rf wave propagation in a magnetized plasma [22]. It uses the (R, Z, ϕ) coordinate system, where R is the major radius and Z the vertical position. The CQL3D code is similar to the LUKE code for electrons with the same system of coordinates, but it can also describe the ion dynamics which is not considered in this paper [21]. Both LUKE and CQL3D codes use identical relativistic collision and quasi-linear velocity space diffusion D_{QL} operators [50, 51]. The methods for calculating D_{QL} from C3PO in LUKE or GENRAY in CQL3D follow a similar approach, and take into account all fragments of rays on a magnetic flux surface with the appropriate wave polarization for each corresponding fragment [16, 21, 23]. A ray may cross several times the same magnetic flux surface. The multiplication of crossings due to the long ray propagation in the weak damping regime may lead to significant wavefield overlapping, which further invalidates RTFP formalism in this regime, unless mechanisms like fast fluctuations of the launched power spectrum are invoked to shorten the rays as described in the present paper. For C3PO/LUKE, the spectral width $\Delta n_\|$ along each ray is equal to its initial value $\Delta n_{\|0}$ associated to each lobe of the launched power spectrum, which results from the Fourier transform of the wave-field structure taking into account the antenna width. Since for a ray tracing, the concept of spectral

[11] The Fourier counterpart of the condition $\lambda \ll d$ is $\Delta n_{\|0} \ll |n_{\|0}|$ which is usually well satisfied for each lobe in the launched power spectrum.

[12] Since the toroidal MHD equilibrium is axisymmetric in the calculations presented in this paper, the C3PO code is used as a 2D ray tracing.

width $\Delta n_{\parallel}$ is irrelevant (infinite plane wave transverse to the ray direction), its evolution along the ray trajectory is arbitrary for calculating the power absorption, which is not true for a beam tracing. Several options have been investigated, like constant width as defined from the antenna size, or an increasing width with $n_{\parallel}$ value along the ray path, etc. It may modify the power absorption of the LH wave and the current drive efficiency for a single ray, as shown in [52]. However, for the 'tail' LH model introduced in section 5, the dependency of $\Delta n_{\parallel}$ has marginal consequences on the LH wave power absorption, as the effective width of the whole power spectrum is generally much larger than $\Delta n_{\parallel}$ itself in the plasma. Recently, it has been shown that reducing $\Delta n_{\parallel}$ down to a very small value may improve LH wave penetration, a particularly important question for LH current drive in reactor grade plasmas [53]. The number of rays in calculations performed by C3PO/LUKE is restricted to one per significant lobe in the launched power spectrum and per poloidal row, as each lobe may be considered as an independent quasi-plane wave [16, 39]. The resonance condition in D_{QL} is decribed by a Gaussian dependence with $n_{\parallel}$, consistently with the launched power spectrum. Conversely, in GENRAY/CQL3D, the resonance condition is described by a boxcar function of width $\Delta n_{\parallel}$. In GENRAY/CQL3D, the power spectrum for each poloidal row is sampled with a set of $n_{\parallel 0}$ values much larger than the number of significant lobes, each $n_{\parallel 0}$ value being an initial condition for a corresponding ray. In this approach, the fraction of power carried by each ray is $P(n_{\parallel 0})\delta n_{\parallel 0}$ where $\delta n_{\parallel 0} \ll \Delta n_{\parallel 0}$. By definition, the effective width $\delta n_{\parallel 0}$ is no more related to the finite size of the antenna in the toroidal direction, but becomes a numerical parameter, which depends on the number of rays considered in the simulation. The mimimum number is rays is prescribed to fill the phase space and make the final result of the RTFP code independent of it, despite the chaotic nature of the ray dynamics that may develop before the wave absorption [54]. It is assumed that the numerical solution converges towards the physical one by increasing the number of rays. Such an approach has led to the development of the LH wave diffusion model which is consistent with the many rays technique, provided the variation of $n_{\parallel}$ remains always incremental along the ray path [55]. While the power flowing along each ray path is integrated from the initial position simultaneously with the ray equations in GENRAY/CQL3D until all the LH power is transferred to the electrons [37], this calculation is performed as a selfconsistent iterative loop in LUKE, from all the ray paths previously calculated by C3PO, the integration time for the rays being much less than the bounce time and the collision time. The D_{QL} and the consistent distribution function are determined after a number of iterations such that the remaining power in each ray is less than 0.1% of the initial value. The first iteration for D_{QL} corresponds to the linear absorption of the LH wave on a Maxwellian plasma, but the final selfconsistent solution for the distribution function and D_{QL} is fully independent of the first guess, as expected, the initial value of D_{QL} deduced from linear absorption being only considered for increasing the quasilinear convergence. When quasilinear effects are taken into account, the full power absorption may take a longer ray length, a consequence of the flattening of the electron velocity distribution function when the quasilinear selconsistency is progressively achieved [16]. Therefore, the modifications of the electron distribution function at different radial positions is the consequence of the interplay between the rays, which itself modifies the power absorption for each ray. The quasilinear selfconsistency links the absorption process of all rays, in momentum but also in configuration spaces. Depending upon plasma conditions, more than one hundred iterations may be necessary, but usually quasilinear convergence is achieved in approximately 20 iterations. Besides the increasing numerical effort with the number of rays considered in a simulation, it has been shown with C3PO/LUKE that the quasilinear convergence is significantly slowed down [52].

Finally, the physics of the LH wave in the SOL, outside the separatrix, is not considered in the C3PO code and a specular reflection is enforced as the LH wave crosses this boundary, such that all rays remain bounded in the core plasma [24]. This approach has minor consequences on the predicted power absorption when the number of reflections is small. However one challenge with the introduction of a SOL model is that it becomes necessary to prescribe the density and temperature in the SOL, which are often not measured accurately. Nevertheless, a SOL model is fully incorporated in GENRAY code, and in this case, the rays are naturally reflected to the plasma core at the LH wave cut-off layer. Collisional damping, which is implemented in both codes, has a marginal impact in C3PO/LUKE calculations, since rays remain always in a region of the plasma where the temperature is high enough to limit parasitic absorption to few percent of the launched power. For GENRAY, the existence of a dense and cold plasma in the SOL may greatly modify current drive predictions, as a large fraction of the launched power spectrum can become non-accessible and the corresponding rays which are propagating over long distances at the periphery have lost a significant part of their power before penetrating into the core region of the plasma [13–15].

The C3PO [LUKE] code has been successfully benchmarked against GENRAY [CQL3D] code for simple reference cases. In addition, for LH current drive in ITER, both C3PO/LUKE and GENRAY/CQL3D give similar power absorption and driven current, with a $\left|n_{\parallel 0}\right|$ dependence consistent with the current drive theory [32, 56]. For these simulations, the LH wave is linearly absorbed before any reflection at the plasma cut-off, such that results are independent of the number of rays (no inter-ray quasilinear coupling).

5. LH current drive simulations

First principle quantitative modeling of LH current drive experiments, using the HXR measurements as the reference diagnostic with magnetic measurements, have been carried out for the Alcator C-Mod tokamak, using GENRAY/CQL3D codes [57]. The intensity of the HXR emission as well as the photon energy dependence were found to be well reproduced for waveguide phasings corresponding to higher values of the parallel refractive index $\left|n_{\parallel 0}^{(0)}\right| = 2.3$–$3.1$, where the spectral

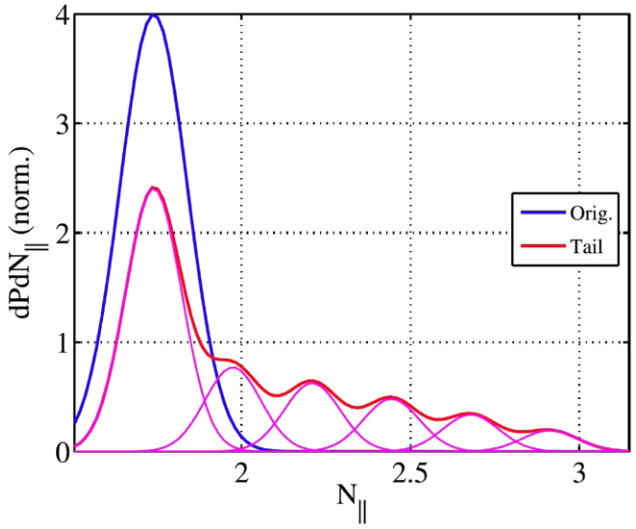

Figure 3. Original Gaussian lobe describing the spectrum in front of the grill, compared to the spectrum at the LCFS constructed using a distribution of spectrally decoupled tail lobes, with 50% of the total power transferred to the tail [72].

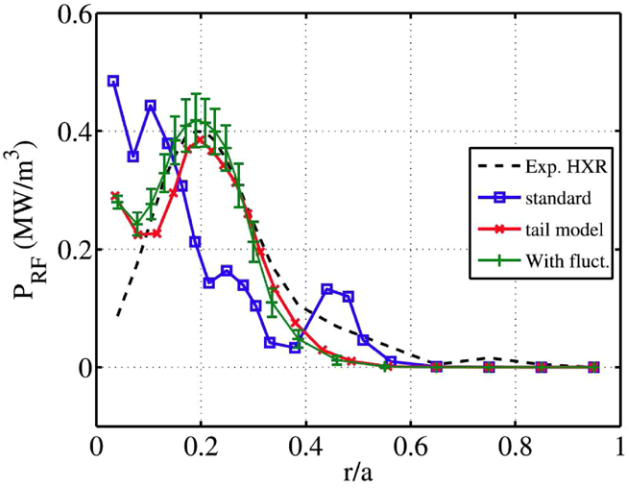

Figure 4. Power deposition profile from standard and tail-model calculations, compared to the radial fast electron bremsstrahlung profile obtained by Abel inversion of the experimental HXR signal in Tore Supra tokamak [16]. The power deposition profile calculated with a fluctuating spectrum is averaged where the time evolution has reached an asymptotic regime. As shown, the fluctuating spectrum at the separatrix or the tail spectrum gives equivalent power absorption profiles.

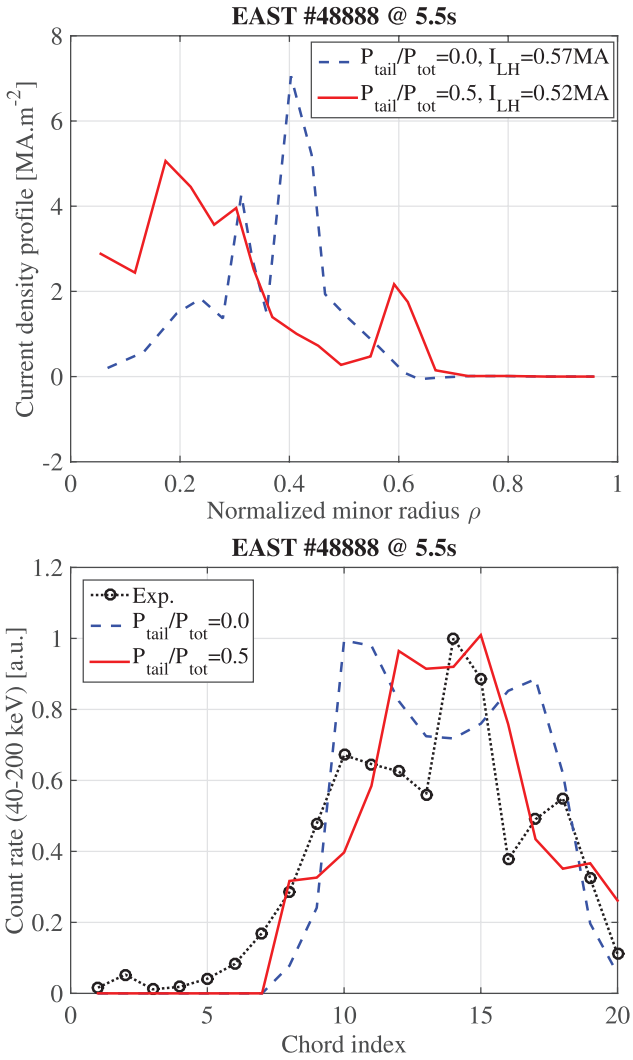

Figure 5. (Top) Current density profile predicted by C3PO/LUKE codes for the full LH current drive LSN diverted discharge in EAST tokamak #48888 at $t = 5.5$ s. Without tail (dashed blue line), the driven current density is well off axis. When 50% of the LH power is transferred to the tail, the current density profile becomes peaked (blue dotted line). No radial transport of the fast electrons is considered in the simulations and collisional damping is negligible. (Bottom) Corresponding normalized line-integrated HXR emission in the photon energy interval 40–200 keV. A good agreement is found with C3PO/LUKE modeling when the tail LH model is considered. A similar agreement may be found with GENRAY/CQL3D by transferring 5% of the LH power at $|n_{\parallel 0}| = 2.7$.

gap is moderate. A similar study has been performed more recently for fully non-inductive discharges with equivalent absorption conditions for the LH wave in the Tore Supra tokamak, using C3PO/LUKE/R5-X2 codes [27]. In this case, the few edge reflections made by rays before full absorption of the LH wave makes the assumptions used for deriving the RTFP equations almost valid, as discussed in section 3. The line-integrated HXR emission is reproduced in the photon energy interval 50–110 keV, as well as the HXR energy spectrum characterized by the photon temperature. As for Alcator C-Mod, a small velocity-dependent radial transport of the form $D_{\psi\psi} = D_{\psi\psi 0}(v_{\parallel}/\hat{v}_{\rm th})H(v_{\parallel} - 3.5\hat{v}_{\rm th})$, with $D_{\psi\psi 0} = 0.1$ m^2 s^{-1}, is considered to smooth out the usual off-axis peak in the power absorption at mid-radius from RTFP, which is never observed experimentally [57, 58]. Simulations are able to reproduce the experimental HXR profiles and their differences with the type of antenna. This is an important result, highlighting the validity of the chain of codes, but also the effectiveness of the toroidal upshift of $n_{\parallel}$ for bridging the spectral gap. The Abel inverted HXR emission is in general relevant from the LH power absorption profile, since fast electrons with the same kinetic energy, but moving in opposite directions along a magnetic field line, have an equivalent contribution to the perpendicular HXR emission [17]. If the LH power spectrum is well asymmetric in $\pm n_{\parallel 0}$, as for the FAM, the Abel inverted HXR profile is a reasonable proxy of the LH driven current

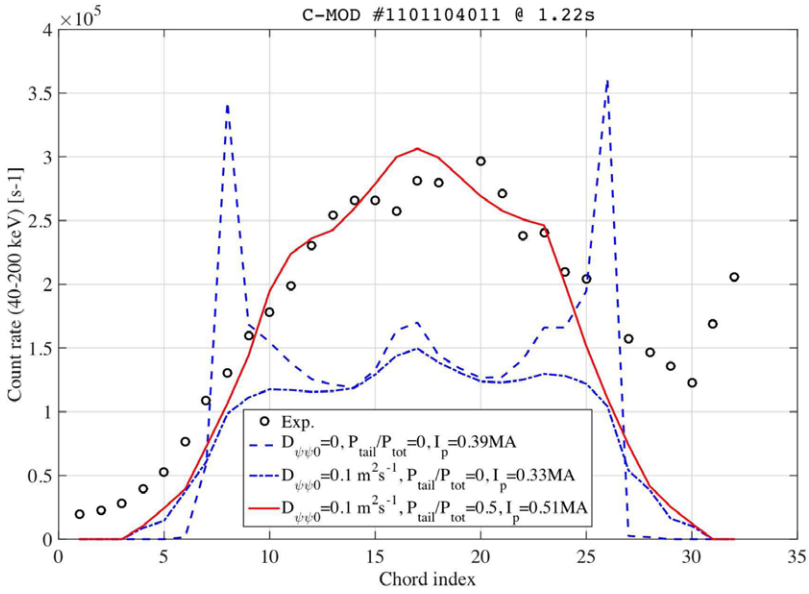

Figure 6. HXR line-integrated profile for the almost full current drive USN Alcator C-Mod diverted discharge #1101104011 at $t = 1.22$ s. Black circles are experimental values obtained with the HXR diagnostic [20]. Without anomalous radial transport for the fast electrons and tail LH model, the predicted profile by C3PO/LUKE/R5-X2 codes is very hollow (dashed blue line). The experimental plasma current is 0.53 MA. A small radial transport of $D_{\psi\psi 0} = 0.1\,\mathrm{m^2\,s^{-1}}$ removes the hollowness of the line-integrated HXR profile, but its shape is not consistent with observations (blue dotted–dashed line). When 50% of the LH power is transferred to the tail, the calculated HXR signal jumps to the correct level, the predicted current is close to the experimental value and the broad experimental profile is well reproduced (red full line). The asymmetric increase of the HXR signal for chords #31 and #32 may be qualitatively ascribed to thick target bremsstrahlung near the divertor.

density profile, as considered in integrated tokamak modeling [59, 60]. The predicted LH current can be highly sensitive to the antenna directivity as compared to HXR profiles. When the electron density in front of the grill is adjusted to fit the measured reflection coefficient [38], it is possible to reproduce simultaneously the HXR profiles and the LH current level, with a consistent evolution of the internal inductance [27]. Such a result is particularly important for the PAM.

Simulations of LH current drive experiments when the spectral gap is large have always been a difficult exercise, because of the possible onset of the chaotic behaviour before the full absorption of the LH wave. This makes predictions sensitive to small variations of any parameters of the simulations [26]. In this regime, the predicted HXR profiles usually disagree with experimental measurements, as shown for the Tore Supra LH full current drive experiment or Alcator C-Mod at a waveguide phase corresponding to $\left|n_{\parallel 0}^{(0)}\right| = 1.55$ [26, 57]. Nevertheless, despite the noise resulting from ray stochasticity, the $n_e^{-3.5}$ experimental scaling law of the HXR emission with the line-averaged density can be reproduced for Tore Supra in the range $n_e = 3 - 5.5 \times 10^{+19}\,\mathrm{m^{-3}}$ [16, 61].

Since density fluctuations at the plasma edge based on the electron drift wave model cannot contribute to bridge efficiently the spectral gap by cumulative rotations of $k_\perp$ along the ray trajectory, as $n_\parallel$ remains unchanged in the scattering process of the LH wave [26], the possibility that the power spectrum could be already very broad at the separatrix has been investigated for large spectral gap LH discharges in Tore Supra [16]. A thorough study with C3PO ray tracing code has shown that introducing a 'tail' in the initial power spectrum described by a set of additional rays while keeping the total launched LH power unchanged (see figure 3), leads to a considerable reduction of the noise in the predictions. With this heuristic LH model, the scaling law of the HXR emission with density can be much more accurately described and, for the first time, the HXR dependence with $\left|n_{\parallel 0}^{(0)}\right|$ is reproduced as well as the HXR profile as shown in figure 4. This remarkable agreement requires that more than half of the total LH power is transferred to the tail, a considerable difference as compared to simplified kinetic calculations that may result from the necessary consistency between the wavefield and the electron distribution function [62, 63]. It is weakly dependent of $P_{\mathrm{tail}}/P_{\mathrm{tot}}$ as far as this ratio remains lower than ~ 0.8 and the upper limit of the tail $n_{\parallel \max}$ is larger than $\widehat{n}_{\parallel L}$. The modified power spectrum considered for initial conditions of ray tracing calculations may be considered as a probability density function (pdf) of a fast fluctuating narrow spectrum with respect to the non-thermal electron slowing down time [16]. Though this model is not yet directly deduced from first principle calculations, the possibility of a spectral broadening at the plasma edge has been considered a long time ago, from parametric instabilities in particular describing LH experiments in JET [42, 64]. Recent full-wave calculations have also shown that fast toroidal fluctuations of the electron density in front of the LH antenna could be an alternative explanation [65].

Considering the successful description of the experimental phenomenology with the tail LH (or equivalently fast fluctuating launched power spectrum) model in Tore Supra, its level of universality has been investigated for LH current drive experiments in EAST and Alcator C-Mod tokamaks. For this purpose, the parameters of the tail LH model obtained from modeling Tore Supra LH experiments as been kept unchanged

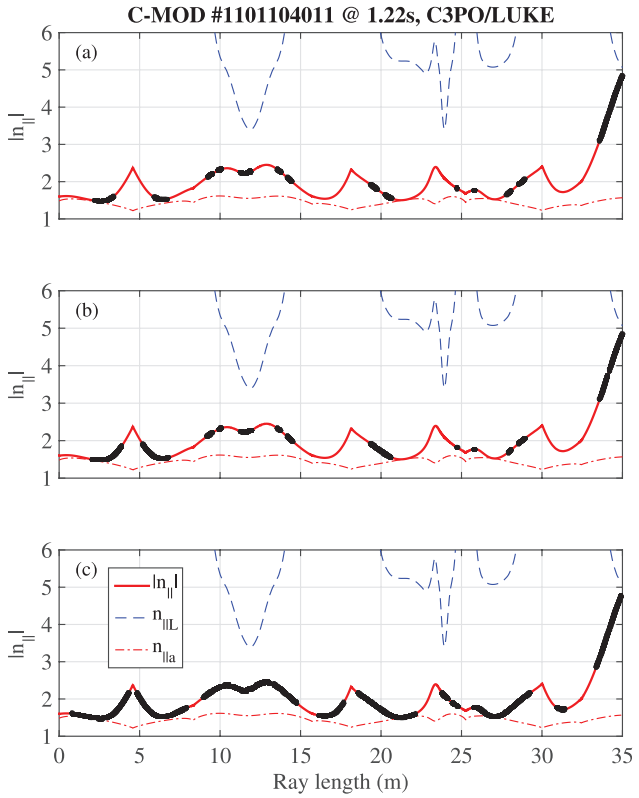

Figure 7. Ray trajectories (full red line) for the same initial conditions $\left|n_{\|0}^{(0)}\right| = 1.55$. The toroidal MHD equilibrium corresponds to the almost full current drive USN Alcator C-Mod diverted discharge #1101104011 at $t = 1.22$ s. (a) standard model, no tail, no fast electron transport, (b) standard model, no tail, small fast electron transport, $D_{\psi\psi 0} = 0.1\,\mathrm{m^2\,s^{-1}}$, (c) 50% of the LH power transferred to the tail and $D_{\psi\psi 0} = 0.1\,\mathrm{m^2\,s^{-1}}$. The blue dashed line corresponds to the strong linear Landau damping condition, and the red dotted dashed line to the Stix–Golant accessibility criterion along the ray trajectory. Black parts along the ray trajectory correspond to the large transfer of power from the wave to the electrons. As the ray propagates near the X-point, the refraction becomes strong leading to a full absorption of the power in the ray. When $P_{\mathrm{tail}}/P_{\mathrm{tot}} = 0.0$, most of the LH power is absorbed at the end of the ray. If $P_{\mathrm{tail}}/P_{\mathrm{tot}} = 0.5$, the transfer of power to the electrons is much more progressive, leading to a better build-up of the fast electron tail, and more central power absorption. The radial transport has a weak effect on power transfer, as shown in (b), even if its contribution is self-consistently calculated with the quasilinear absorption.

[16]. A fully non-inductive diverted discharge at a line-averaged density $\overline{n}_e = 2.5 \times 10^{+19}\ \mathrm{m^{-3}}$ performed in the EAST tokamak is first considered (Lower Single Null, LSN), where 2.25 MW of LH power at 4.6 GHz drives about 0.39 MA (discharge #48888 at $t = 5.5$ s). The core electron temperature reaches 3 keV in the steady-state regime without evidence of sawtooth activity, and the estimated internal inductance $l_i \simeq 1.22$ is almost unchanged as compared to the Ohmic phase within the error bars. As shown in figure 5, the power absorption predicted by C3PO/LUKE is off-axis when $P_{\mathrm{tail}}/P_{\mathrm{tot}} = 0$, with a predicted plasma current of 0.57 MA higher than the experimental level. Predictions obtained with GENRAY/CQL3D and TORLH fullwave codes are similar [28]. In this case, the calculated HXR profile is hollow, in disagreement with observations as shown in figure 5. Conversely, with $P_{\mathrm{tail}}/P_{\mathrm{tot}} = 0.5$, the LH current density profile is much more central and broad, and the predicted LH current is slightly reduced to 0.52 MA. In this case, the calculated current density profile becomes close to the toroidal MHD equilibrium one, which is consistent with the measured internal inductance and the lack of sawtooth $q_0 > 1$. In order to retrieve the lower level of the plasma current, a large radial diffusion of the fast electrons must be introduced in the calculations, $D_{\psi\psi 0} \simeq 2.0$ $\mathrm{m^2\,s^{-1}}$. However, given the large uncertainty about the calculated LH current arising from the directivity of multijunctions as shown in [27], the difference between observations may not result from a transport effect, which, moreover, is not sufficient to peak the predicted current profile when $P_{\mathrm{tail}}/P_{\mathrm{tot}} = 0$. Further quantitative studies are necessary to clarify this point.

A similar study has been carried out for the upper single null (USN) diverted Alcator C-Mod discharge #1101104011 at $t = 1.22$ s. With 0.63 MW at 4.6 GHz associated to the main lobe at $\left|n_{\|0}^{(0)}\right| = 1.55$ in the LH power spectrum, the plasma current reaches 0.53 MA, and the Ohmic loop voltage falls down to 75 mV. The line-averaged density is $\overline{n}_e = 4.5 \times 10^{+19}\ \mathrm{m^{-3}}$. From C3PO/LUKE calculations, the Ohmic contribution to the total plasma current is about 20%. An effective charge $Z_{\mathrm{eff}} = 1.8$ is considered, taking into account in HXR calculations that it is dominated by a high-Z impurity (molybdenum) [17]. With $P_{\mathrm{tail}}/P_{\mathrm{tot}} = 0$, the predicted plasma current is 0.39 MA, including synergistic effects between the LH driven current and the Ohmic field. As shown in figure 6, the predicted line-integrated HXR profile is strongly hollow, while it is broad and peaked experimentally. With $D_{\psi\psi 0} = 0.1$ $\mathrm{m^2\,s^{-1}}$, the sharp peaks in the HXR profiles corresponding to the strongly localised absorption of the LH power at mid radius are smoothed out like for Tore Supra LH current drive simulations [27]. However, the shape of the predicted line-integrated HXR profile is much too flat, a discrepancy with observations that cannot be compensated for by increasing the fast electron radial transport because the predicted plasma current becomes much too small. Conversely, with $P_{\mathrm{tail}}/P_{\mathrm{tot}} = 0.5$, the HXR is significantly larger, with the correct bell shape for the HXR profile. The predicted current reaches 0.51 MA, very close to the experimental level. By increasing $P_{\mathrm{tail}}/P_{\mathrm{tot}}$ to 0.75, this good general agreement remains, which confirm the robustness of the tail LH model observed for Tore Supra simulations [16]. A detailed analysis for a ray centered on the main lobe at $\left|n_{\|0}^{(0)}\right| = 1.55$ shows that the transfer of power from the wave to the electrons is much more progressive along the ray path with the tail LH model, leading to a more central absorption combined with a full build-up of the fast electron tail in momentum space (see figure 7). This result points out the importance of the self-consistency between the wavefield and the electron distribution function in the determination of the power absorption of the LH wave and the current drive efficiency. Indeed, for the studied case, the broadening of the launched power spectrum at the plasma edge has not led to the standard reduction of the LH driven current [66]. The interplay between dynamics of the LH wave in momentum and configuration spaces is critical.

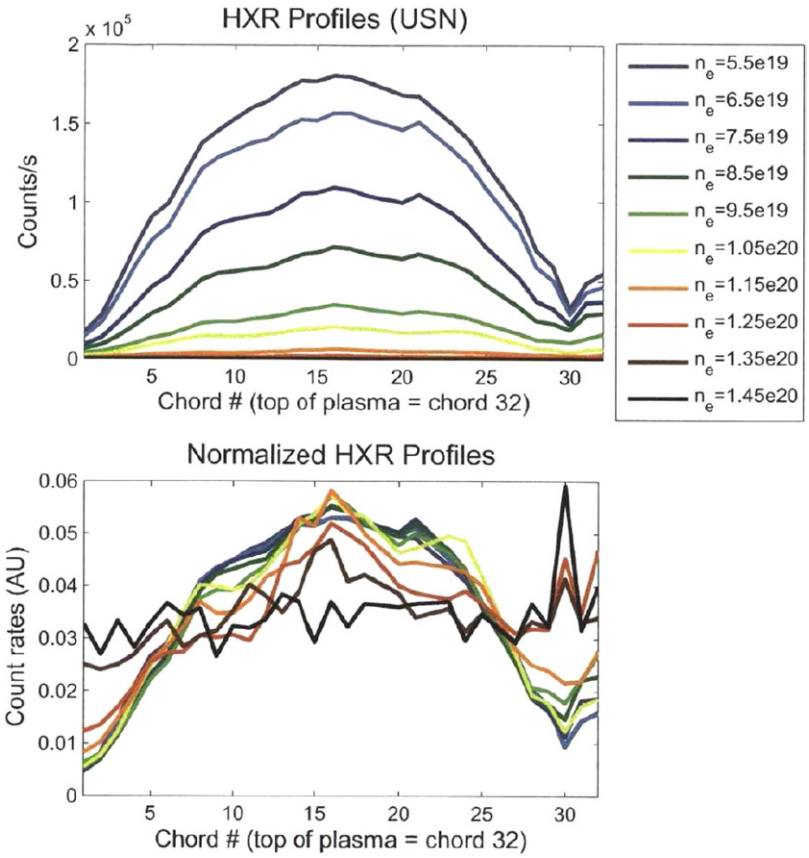

Figure 8. HXR profiles for varying density (USN Alcator C-Mod diverted discharges), taken from shots 1080429003/4/7/8/9/14/15/16/17/18, and 1080513006/7/15/16/22/23/24 from [67]. Densities in the legend are line-averaged. In these discharges, $\left|n_{\|0}^{(0)}\right| \simeq 1.9$, $B = 5.4$ T, and $I_p \simeq 800$ kA. The upper plot shows count rates and the lower plot shows count rates normalized to the total count rate (on all chords). In USN, a 'shoulder' feature appears in the HXR profiles at the top of the plasma. This shoulder becomes more prominent in the normalized HXR profiles at higher densities.

As shown in figure 8, the measured line-integrated HXR profiles have an identical shape until the line-averaged density exceeds $\overline{n}_e = 1.15 \times 10^{+20}\ m^{-3}$, which is similar to the predicted one by the tail LH model. Above, a strong flattening is observed, with an enhanced emission localized to central chords only [67]. This evolution suggests a change in the LH dynamics at very high plasma densities, and in this case the first down-shifted side-bands become comparable to the pump power for the ion cyclotron parametric decay signal [68]. This statement is confirmed by studying the scaling of the HXR emission with density for $\left|n_{\|0}^{(0)}\right| = 1.95, B_t = 5.4\,\mathrm{T}$ and $I_p = 0.83$ MA [14]. For this purpose, the Alcator C-Mod discharge #1080513016 is considered, where $\overline{n}_e = 1.3 \times 10^{+20}$ m^{-3} at $t = 1.06$ s. The power launched in the main lobe is 0.53 MW and the loop voltage is large, about 1.45 V. C3PO/LUKE calculations show that the plasma current is almost fully driven by the Ohmic power, while the LH fraction, reaching only 25 kA, is generated far from the magnetic axis at $\rho \geqslant 0.6$. Even if collisional damping is taken into account, its contribution remains almost negligible to the modeling results. Simulations are also performed with $D_{\psi\psi 0} = 0.1$ m^2 s^{-1}, but the results are weakly dependent of the radial transport at this high collisionality [58]. The Ohmic electric field profile is assumed to be flat. Nevertheless, synergistic effects at the radial location where the LH wave is absorbed remain weak for $P_{\mathrm{tail}}/P_{\mathrm{tot}} = 0$, because the absorption occurs after a strong upshift of $|n_{\|}|$ in the vicinity of the X-point, as discussed in section 2 and shown in figures 1 and 7. Electrons of the tail driven by the LH wave have therefore a moderate kinetic energy as compared to those of the thermal bulk, and their high collisionality makes them weakly sensitive to an Ohmic electric field. In this case, the predicted HXR emission is very low, in agreement with experimental measurements. Conversely, with $P_{\mathrm{tail}}/P_{\mathrm{tot}} = 0.5$, the absorption is much more progressive during the propagation, leading to a more developed fast electron tail in the plasma and an enhanced sensitivity to the Ohmic electric field. The fast fluctuations of the launched power spectrum at the plasma edge lead to a predicted HXR emission that is larger by one order of magnitude, well above experimental observations. RTFP calculations are therefore consistent with the variations of the experimental line-integrated HXR profiles when the density is increased, which suggests that the tail LH model is no longer valid above $\overline{n}_e \simeq 1.0 \times 10^{+20}$ m^{-3}.

Since almost all the plasma current is driven by the Ohmic field, the effect of electron density on the HXR emission can be qualitatively estimated from the Alcator C-Mod discharge #1080513016, assuming that the toroidal MHD equilibrium remains almost unchanged. In this approach, the kinetic pressure is supposed to be constant, a reasonable assumption for Ohmic discharges. As shown in figure 9, the large rise of the

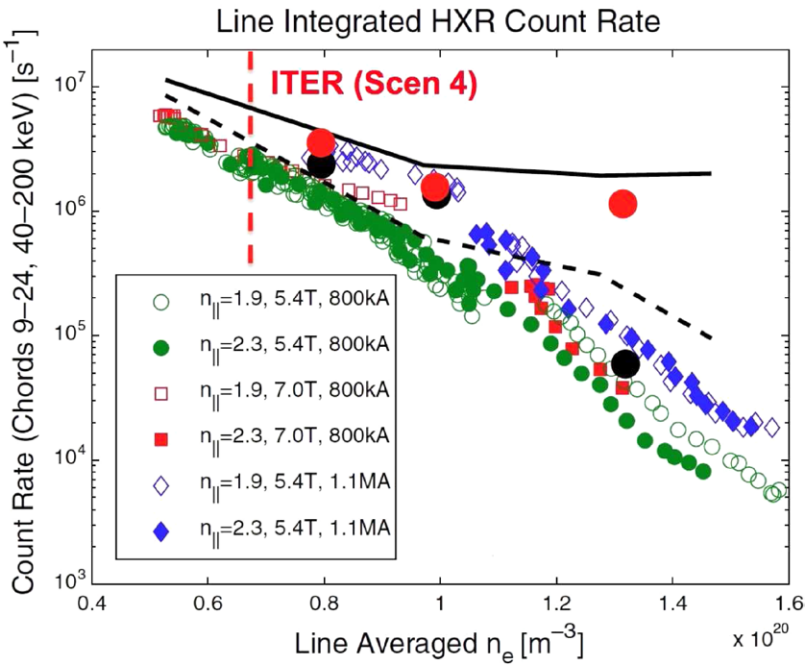

Figure 9. HXR count rate in the photon energy range 40–200 keV, summed over the cords #9 to #24 as a function of the line-averaged electron density for the Alcator C-Mod tokamak (USN diverted configuration). The full black line corresponds to GENRAY/CQL3D calculations without collisional damping of the LH wave in the SOL. When this effect is taken into account, GENRAY/CQL3D precictions are considerably closer to experimental results, leading to a reduction of the HXR emission by an order of magnitude above $n_e = 10^{+20}$ m^{-3} [14]. The full black circles correspond to the C3PO/LUKE simulations, taking into account the toroidal refraction only. When fluctuations of the power spectrum at the separatrix are considered (full red circles) the predicted HXR signal is similar up to $n_e = 10^{+20}$ m^{-3} but larger than observations at higher densities. The dotted red line indicates the line-averaged density for the ITER reference scenario IV [3].

HXR emission by lowering the density is well reproduced using C3PO/LUKE codes. It results from the increase of the temperature, which has a strong effect since the wave absorption is almost linear. Besides the reduction of the plasma collisionality, more fast electrons can be driven by the LH wave at a fixed power level. Since the tail of fast electrons is well formed in this case, the results obtained with a fluctuating power spectrum at the plasma edge are very similar. Therefore, while simulations with GENRAY/CQL3D codes ascribe the decrease of the line-integrated HXR emission with density to the parasitic absorption of the LH wave in the SOL by collisional damping, an alternative interpretation may be given using C3PO/LUKE/R5-X2 codes. Interestingly, above $\overline{n}_e = 1.0 \times 10^{+20}$ m^{-3}, GENRAY/CQL3D codes without collisional damping and C3PO/LUKE with the tail LH model gives a similar HXR emission level, as shown in figure 9. This points out how the difference of use between the two codes may deeply impact the interpretation, and the role played by the number of rays in the simulations must be clarified.

The broadening of the LH power spectrum at the plasma edge has been considered a long time ago, in particular for parametric instabilities describing non-linear mode-coupling [69]. Other mechanisms may also contribute to this effect, like LH wave diffraction by a fast fluctuating density in a thin layer in front of the antenna. By symmetry, the perturbation must be along the toroidal direction [65]. Fast random shift between the antenna waveguides resulting from a fluctuating neutral ionization may also provide a qualitative explanation. The latter could explain the disappearance of the power spectrum fluctuations at very high density, but more refined experimental investigations are necessary.

Since the line-averaged density of the ITER design scenario IV is about $\overline{n}_e = 6.5 \times 10^{+19}$ m^{-3}, fast fluctuations of the power spectrum at the separatrix can potentially impact current drive predictions according to C3PO/LUKE calculations [3]. For $n_{\parallel \max} = \widehat{n}_{\parallel L}$, no effect can occur, since in that case $\left|n_{\parallel 0}^{(0)}\right| > n_{\parallel \max}$, as shown in figure 2. Conversely, if $n_{\parallel \max} = 3$, while keeping $P_{\rm tail}/P_{\rm tot} = 0.5$, the predicted LH current drops from 0.68 MA to 0.53 MA when 20 MW of LH power is injected at $\left|n_{\parallel 0}^{(0)}\right| = 2.0$. This represents a reduction of 20% of the current drive efficiency, as compared to the value estimated from standard calculations [3]. The power absorption is broader but the radial penetration remains still bounded by the strong linear damping at $\rho \approx 0.7$. In this case, some energetic electrons are found to be generated in the vicinity of the separatrix. Finally, even if collisional damping is strong in the SOL, its impact LH current predictions for ITER is likely weak, as absorption is achieved in single pass. These results point out the weakness of the extrapolation capability of the current drive efficiency for reactor-grade plasmas as predictions may strongly depend of the spectral properties of the LH wave at the plasma periphery. Conversely, the location of the power absorption of the LH wave is rather robust, a direct consequence of the penetration barrier resulting from linear absorption by a thermal plasma at high temperature. Therefore, even if the agreement between modeling and experiments in existing tokamaks has improved significantly,

conclusions drawn may not necessarily be valid for reactor-grade plasmas. It is therefore critical to perform LH experiments for which single pass absorption is effectively achieved, in order to assess the role of the launched power spectrum and the dynamics of the LH wave in the SOL with available powerful diagnostics, even if in existing tokamaks, the LH current drive efficiency may be significantly lower [70].

6. Conclusions

Quantitative simulations of LH driven discharges have become a standard in modeling, and are essential for an accurate physics assessment. When the spectral gap is moderate, LH simulations based on standard toroidal refraction are in quantitative agreement with the non-thermal bremsstrahlung emission (HXR) profiles and the plasma current. However, the LH current may be sensitive to the antenna directivity while HXR profiles are more robust and relevant to the power absorption in general. For large spectral gap conditions, fast fluctuations of the power spectrum (tail LH model) lead to an improved quantitative agreement between observations and simulations using C3PO/LUKE RTFP code. The predictions are much less noisy and variations of HXR emission with density and $\left|n_{\|0}^{(0)}\right|$ can be well reproduced for Tore Supra tokamak, as well as the Abel inverted HXR profile. This heuristic model leads also to an improved quantitative agreement with experimental observations for full current drive diverted discharges in the EAST and Alcator C-Mod tokamaks. Fluctuations of the power spectrum at the separatrix lead to a more progressive power absorption of the LH wave as it propagates in the plasma and a well developed tail of non-thermal electrons by Landau damping. The power absorption is therefore more central, especially for diverted magnetic configurations which are particularly favorable for a strong off-axis refraction, which is not observed experimentally up to $\overline{n}_e = 1.0 \times 10^{+20}$ m^{-3} in Alcator C-Mod tokamak. Above this, calculations with C3PO/LUKE codes using the tail LH model overestimate the HXR emission, but variations of the line-integrated HXR profiles with density in the Alcator C-Mod tokamak clearly indicate a change of regime for the LH wave dynamics. While GENRAY/CQL3D codes explain quantitatively the scaling law of the HXR emission with density by an increasing collisional damping in the SOL and near the divertor, a different interpretation is provided by C3PO/LUKE simulations. At very high density, the strong refraction of the LH wave near the X-point makes the power absorption almost linear, and therefore very sensitive to the plasma temperature. If the power spectrum at the separatrix is broad, the power absorption of the LH wave in ITER is modified and the current drive efficiency is reduced with a slightly more off-axis power absorption. Conversely, the impact of collisional damping is likely marginal because of single pass absorption. ITER-relevant experiments in existing machines that correspond to almost single pass absorption must be carried out to clarify the different interpretations and improve extrapolation capabilities for reactor-grade plasmas. The WEST tokamak will be a powerful tool for this purpose [71]. Whatever the LH model, the role of the SOL in the core LH physics is likely to be very important.

References

[1] Tuccillo A A *et al* 2005 Progress in LHCD: a tool for advanced regimes on ITER *Plasma Phys. Control. Fusion* **47** B363–77

[2] Hoang G T *et al* 2009 A lower hybrid current drive system for ITER *Nucl. Fusion* **49** 075001

[3] Decker J *et al* 2011 Calculations of lower hybrid current drive in ITER *Nucl. Fusion* **51** 073025

[4] Pericoli Ridolfini V *et al* 2005 LHCD and coupling experiments with an ITER-like PAM launcher on the FTU tokamak *Nucl. Fusion* **45** 1085–93

[5] Ekedahl A *et al* 2010 Validation of the ITER-relevant passive-active-multijunction LHCD launcher on long pulses in Tore Supra *Nucl. Fusion* **50** 112002

[6] Ekedahl A *et al* 2012 Influence of gas puff location on the coupling of lower hybrid waves in jet ELMY H-mode plasmas *Plasma Phys. Control. Fusion* **54** 074004

[7] Kirov K K, Baranov Y, Mailloux J, Mayoral M-L, Nave M F F, Ongena J and JET EFDA Contributors 2010 LH power deposition and CD efficiency studies by application of modulated power at JET *Nucl. Fusion* **50** 075003

[8] Goniche M *et al* 2010 Lower hybrid current drive for the steady-state scenario *Plasma Phys. Control. Fusion* **52** 124031

[9] Pericoli Ridolfini V, Apicella M L, Calabro G, Cianfarani C, Giovannozzi E and Panaccione L 2011 Lower hybrid current drive efficiency in tokamaks and wave scattering by density fluctuations at the plasma edge *Nucl. Fusion* **51** 113023–35

[10] Kirov K K, Baranov Y, Gerbaud T, Goniche M, Mailloux J, Mayoral M L, Ongena J, Schmuck S and JET EFDA Contributors 2012 Analysis of electron cyclotron emission by fast electrons generated by lower hybrid current drive at JET *Plasma Phys. Control. Fusion* **54** 074003

[11] Ding B J *et al* 2013 Experimental investigations of LHW plasma coupling and current drive related to achieving H-mode plasmas in EAST *Nucl. Fusion* **53** 113027

[12] Barbato E, Saveliev A, Voitsekhovitch I, Kirov K, Goniche M, the ISM ITER Scenario Modeling Group and JET EFDA Contributors 2014 Time-dependent simulation of lower hybrid current drive in JET discharges *Nucl. Fusion* **54** 123009

[13] Wallace G M *et al* 2010 Absorption of lower hybrid waves in the scrape off layer of a diverted tokamak *Phys. Plasmas* **17** 082508

[14] Wallace G M *et al* 2011 Lower hybrid current drive at high density in Alcator C-Mod *Nucl. Fusion* **51** 083032

[15] Barbato E 2011 The role of non-resonant collision dissipation of lower hybrid current driven plasmas *Nucl. Fusion* **51** 103032

[16] Decker J, Peysson Y, Artaud J-F, Nilsson E, Ekedahl A, Goniche M, Hillairet J and Mazon D 2014 Damping of lower hybrid waves in large spectral gap configurations *Phys. Plasmas* **21** 092504

[17] Peysson Y and Decker J 2008 Fast electron bremsstrahlung in axisymmetric magnetic configuration *Phys. Plasmas* **15** 092509

[18] Peysson Y and Imbeaux F 1999 Tomography of the fast electron bremsstrahlung emission during lower hybrid current drive on TORE SUPRA *Rev. Sci. Instrum.* **70** 3987–4007

[19] Tudisco O *et al* 2004 The diagnostic systems in the FTU *Fusion Sci. Technol.* **45** 402–21

[20] Liptac J, Parker R, Tang V, Peysson Y and Decker J 2006 Hard x-ray diagnostic for lower hybrid experiments on Alcator C-Mod *Rev. Sci. Instrum.* **77** 103504

[21] Harvey R W and McCoy M G 1992 The CQL3D Fokker–Planck code *AEA Technical Committee on Advances in Simulation and Modeling of Thermonuclear Plasmas* pp 489–526

[22] Smirnov A P and Harvey R W 1995 Calculations of the current drive in diii-d with the genray ray tracing code *Bull. Am. Phys. Soc.* **40** 1837 *(37th Annual Meeting of the Division of Plasma Physics* (*Louisville, Kentucky*, *6–10 November 1995)* abstract 8 p 35)

[23] Decker J and Peysson Y 2004 DKE: a fast numerical solver for the 3D drift kinetic equation *Report* EUR-CEA-FC-1736 (Euratom-CEA)

[24] Peysson Y, Decker J and Morini L 2012 A versatile ray-tracing code for studying rf wave propagation in toroidal magnetized plasmas *Plasma Phys. Control. Fusion* **54** 045003

[25] Shiraiwa S *et al* 2013 Progress towards steady-state regimes in Alcator C-Mod *Nucl. Fusion* **53** 113028

[26] Peysson Y, Decker J, Morini L and Coda S 2011 Rf current drive and plasma fluctuations *Plasma Phys. Control. Fusion* **53** 124028

[27] Nilsson E *et al* 2013 Comparative modelling of lower hybrid current drive with two launcher designs in the Tore Supra tokamak *Nucl. Fusion* **53** 083018

[28] Yang C, Bonoli P T, Wright J C, Ding B J, Parker R, Shiraiwa S and Li M H 2014 Modelling of the EAST lower-hybrid current drive experiment using GENRAY/CQL3D and TORLH/CQL3D *Plasma Phys. Control. Fusion* **56** 125003

[29] Bonoli P T *et al* 2008 Lower hybrid current drive experiments on Alcator C-Mod: comparison with theory and simulation *Phys. Plasmas* **15** 056117

[30] Wright J C, Bonoli P T, Schmidt A E, Phillips C K, Valeo E J, Harvey R W and Brambilla M A 2009 An assessment of full wave effects on the propagation and absorption of lower hybrid waves *Phys. Plasmas* **16** 072502

[31] Bonoli P T 2014 Review of recent experimental and modeling progress in the lower hybrid range of frequencies at iter relevant parameters *Phys. Plasmas* **21** 061508

[32] Fisch N J 1987 Theory of current drive in plasmas *Rev. Mod. Phys.* **59** 175–234

[33] Brambilla M 1976 Slow-wave launching at the lower hybrid frequency using a phased waveguide array *Nucl. Fusion* **16** 47–54

[34] Ding B *et al* 2011 Recent results of LHCD experiments in EAST *Plasma Sci. Technol.* **13** 153–6

[35] Wallace G M *et al* 2013 Advances in lower hybrid current drive technology on Alcator C-Mod *Nucl. Fusion* **53** 073012

[36] Bonoli P T 1984 Linear theory of lower hybrid heating *IEEE Trans. Plasma Sci.* **PS-12** 95–107

[37] Bonoli P T and Englade R C 1986 Simulation model for lower hybrid current drive *Phys. Fluids* **29** 2937–50

[38] Hillairet J, Voyer D, Ekedahl A, Goniche M, Kazda M, Meneghini O, Milanesio D and Preynas M 2010 Aloha: an advanced lower hybrid antenna coupling code *Nucl. Fusion* **50** 125010

[39] Cairns R A and Fuchs V 2010 Calculation of a wave field from ray tracing *Nucl. Fusion.* **50** 095001

[40] Peysson Y, Sébelin E, Litaudon X, Moreau D, Miellou J C, Shoucri M and Shkarofsky I P 1998 Full wave modelling of the lower hybrid current drive in tokamaks *Nucl. Fusion* **38** 939–44

[41] Brambilla M 1998 *Kinetic Theory of Plasma Waves* (Oxford: Oxford Science Publications)

[42] Cesario R, Cardinali A, Castaldo C, Paoletti F and Mazon D 2004 Modeling of a lower-hybrid current drive by including spectral broadening induced by parametric instability in tokamak plasmas *Phys. Rev. Lett.* **92** 175002

[43] Paoletti F, Ignat D W, Kesner J, Bernabei S, Kaita R, Leblanc B, Levinton F M and Luckhardt S C 1994 Lower hybrid current drive accessibility study with reconstructed magnetic equilibria in pbx-m *Nucl. Fusion* **34** 771–6

[44] Takahashi H 1994 The generalized accessibility and spectral gap of lower hybrid waves in tokamaks *Phys. Plasmas* **1** 2254–76

[45] Cesario R, Cardinali A, Castaldo C, Paoletti F, Fundamenski W, Hacquin S and the JETEFDA workprogramme contributors 2006 Spectral broadening of lower hybrid waves produced by parametric instability in current drive experiments of tokamak plasmas *Nucl. Fusion* **46** 462–76

[46] Peysson Y and Decker J 2008 Calculation of rf current drive in tokamaks *Theory of Fusion Plasmas* (*AIP Conf. Proc.* vol 1069) ed X Garbet *et al* pp 176–87 *(Joint Varenna-Lausanne Int. Workshop on Theory of Fusion Plasmas (Varenna, Italy*, *25–29 August 2008))*

[47] Shiraiwa S, Meneghini O, Parker R, Bonoli P, Garrett M, Kaufman M C, Wright J C and Wukitch S 2010 Plasma wave simulation based on a versatile finite element method solver *Phys. Plasmas* **17** 056119

[48] Peysson Y and Decker J 2014 Numerical simulations of the radio-frequency driven toroidal current in tokamaks *Fusion Sci. Technol.* **65** 22–42

[49] Richardson A S, Bonoli P T and Wright J C 2010 The lower hybrid wave cutoff: a case study in eikonal methods *Phys. Plasmas* **17** 052107–18

[50] Kennel C F and Engelmann F 1966 Velocity space diffusion from weak plasma turbulence in a magnetic field *Phys. Fluids* **9** 2377–87

[51] Lerche I 1968 Quasilinear theory of resonant diffusion in a magneto-active relativistic plasma *Phys. Fluids* **11** 1720–6

[52] Decker J and Peysson Y 2006 On self-consistent simulation of the lower hybrid current drive *33rd EPS Conf. on Plasma Physics and Controlled Fusion*

[53] Amicucci L *et al* 2016 *Plasma Phys. Control. Fusion* **58** 014042

[54] Bizarro J P and Moreau D 1993 On ray stochasticity during lower hybrid current drive in tokamaks *Phys. Fluids* B **5** 1227–38

[55] Kupfer K, Moreau D and Litaudon X 1993 Statistical theory of wave propagation and multipass absorption for current drive in tokamaks *Phys. Fluids* B **5** 4391–407

[56] Bonoli P T *et al* 2006 Benchmarking of lower hybrid current drive codes with application to ITER-relevant regimes *Fusion Energy Proc. 21st Int. Conf. Chengdu* (*Vienna: IAEA*) CD-ROM file IT/P1-2 (www-naweb.iaea.org/napc/physics/FEC/FEC2006/html/index.htm)

[57] Schmidt A, Bonoli P T, Meneghini O, Parker R R, Porkolab M, Shiraiwa S, Wallace G, Wright J C, Harvey R W and Wilson J R 2011 Investigation of lower hybrid physics through power modulation experiments on Alcator C-Mod *Phys. Plasmas* **18** 056122

[58] Peysson Y 1993 Transport of fast electrons during LHCD in TS, JET and ASDEX *Plasma Phys. Control. Fusion* **35** B253–62

[59] Peysson Y and the Tore Supra Team 2001 High power lower hybrid current drive experiments in the Tore Supra tokamak *Nucl. Fusion* **41** 1703–13

[60] Artaud J F *et al* 2010 The CRONOS suite of codes for integrated tokamak modelling *Nucl. Fusion* **50** 043001

[61] Goniche M *et al* 2013 Lower hybrid current drive at high density on Tore Supra *Nucl. Fusion* **53** 033010

[62] Succi S, Appert K, Muschietti L, Vaclavik J and Wersinger J M 1984 On the generation of superthermal electrons in lower-hybrid current-drive experiments *Phys. Lett.* A **106A** 137–9
[63] Succi S, Appert K and Vaclavik J 1985 Generation of superthermal electrons interacting with lower hybrid waves revisited *Plasma Phys. Control. Fusion* **27** 863–71
[64] Cesario R, Amicucci L, Castaldo C, Kempenaars M, Jachmich S, Mailloux J, Tudisco O, Galli A, Krivska A and JET-EFDA contributors6 2011 Plasma edge density and lower hybrid current drive in JET (joint european torus) *Plasma Phys. Control. Fusion* **8** 085011
[65] Madi M, Peysson Y, Decker J and Kabalan K Y 2015 Propagation of the lower hybrid wave in a density fluctuating SOL *Plasma Phys. Control. Fusion* **57** 125001
[66] Ehst D A and Karney C F F 1991 Approximate formula for radiofrequency current drive efficiency with magnetic trapping *Nucl. Fusion* **31** 1933–8
[67] Schmidt A 2011 Modeling of lower hybrid driven fast electrons on Alcator C-Mod *PhD Thesis* Massachusetts Institute of Technology
[68] Baek S G, Parker R R, Shiraiwa S, Wallace G M, Bonoli P T, Brunner D, Faust I C, Hubbard A E, LaBombard B and Porkolab M 2013 Measurements of ion cyclotron parametric decay of lower hybrid waves at the high-field side of Alcator C-Mod *Plasma Phys. Control. Fusion* **55** 052001
[69] Cesario R *et al* 2014 Spectral broadening of parametric instability in lower hybrid current drive at a high density *Nucl. Fusion* **54** 043002
[70] Leuterer F *et al* 1986 Influence of the NPAR spectrum on lower hybrid current drive in ASDEX *Europhysics Conf. Abstracts* vol 10C pp 409–12
[71] Bourdelle C *et al* 2015 West physics basis *Nucl. Fusion* **55** 063017
[72] Delpech L *et al* 2014 Advances in multi-megawatt lower hybrid technology in support of steady-state tokamak operation *Nucl. Fusion* **54** 103004